INTENSITY DISTRIBUTIONS IN FRAUNHOFER MULTIPLE SLIT DIFFRACTION PATTERNS

Thesis for the Degree of M. S.

MICHIGAN STATE COLLEGE

Albert Ernest Smith

1951

This is to certify that the

thesis entitled

INTENSITY DISTRIBUTIONS IN FRAUNHOFER MULTIPLE SLIT DIFFRACTION PATTERNS

presented by

Albert Ernest Smith

has been accepted towards fulfillment
of the requirements for

M.S. degree in Physics

C. W. Hause
Major professor

Date May 18, 1951

O-169

INTENSITY DISTRIBUTIONS IN FRAUNHOFER MULTIPLE SLIT DIFFRACTION PATTERNS

by

Albert Ernest Smith

A Thesis

Submitted to the School of Graduate Studies of Michigan State College of Agriculture and Applied Science in partial fulfillment of the requirements for the degree of

MASTER OF SCIENCE

Department of Physics

1951

ACKNOWLEDGMENT

I wish to express my sincere appreciation to Professor C. D. Hause for the suggestion of this problem and for encouragement and helpful direction toward its completion.

Albert E. Smith

TABLE OF CONTENTS

I. INTRODUCTION

The applications of Fraunhofer diffraction patterns have been many and varied.

The diffraction patterns from rectangular and circular apertures give a means of determining the ultimate detail which may be expected in the images produced by optical instruments with apertures of this type.

The two-slit system yields a method for determining the angular width of a small source. In this method, which was developed by Michelson,[1] use is made of the fact that the diffraction pattern from a very small source is made up of equally spaced maxima and minima. If two line sources are displaced slightly with respect to each other, the intensity distribution in the resulting diffraction pattern is the sum of the intensities in the individual patterns.

It was found by Michelson that if the light source consists of two separate slits which subtend an angle α at the diffracting apertures and if $\alpha = \frac{1}{2}\frac{\lambda}{d}$, the resultant pattern no longer shows maxima and minima of intensity, but has a constant intensity for all angles of diffraction. λ is the wavelength of light used and d is the separation of the diffracting slits.

In this method use is made of the fact that two separate line sources are incoherent with respect to each other. For this reason the resulting intensity distribution in the diffraction pattern is the sum of the intensity distributions from the individual sources.

If the source used is a solid rectangle, it may be regard-

ed as a large number of line sources, and the result is an incoherent source. It has been found here that the maxima and minima in the resulting pattern disappear when $\alpha = \frac{\lambda}{d}$, where α is the angle subtended by the width of the source at the diffracting slits. In the case of a solid disk source, the fringes are found to disappear when the diameter subtends an angle $\alpha = \frac{1.22\ \lambda}{d}$.

Calculations are also carried out by Michelson for a disk source in which the illumination decreases toward the perimeter and for two separated disk sources where the separation is large in comparison with the diameter of either source.

These results have been applied to the determination of the diameters of double stars,[2] to the separation of double stars,[3] and to the measurement of the diameters of microscopic particles.[4]

Since in all these cases the intensity distribution in the two-slit diffraction pattern has been used as a characteristic which would allow assignment of source dimensions, it is of interest to determine whether by adding slits between these two the effective resolving power of the area in which the two slits are located may be increased.

The term <u>resolving power</u>, as it is used in this paper, is defined as the smallest angle of source, subtended at the diffracting apertures, to which dimensions may be assigned. It is assumed that the overall dimensions of the diffractor do not increase beyond a certain limit.

The purpose, then, of this paper has been to determine whether the inclusion of additional slits between the original two increases the effective resolving power of the area, that is, whether

dimensions may be accurately assigned to smaller angles than those to which dimensions are assignable by the use of the two slits.

It has been found that when three slits are used an effective increase in resolving power of 33% is achieved. When four slits are used, an effective increase of the order of 25% is gained. The four-slit case is found to be more precise experimentally than the three-slit.

Calculations are carried out for the case of a rectangular source and for the case of a disk source.

II. SLIT SOURCE

It has been found[5] that when light of wavelength λ emanating from a line source is diffracted by N rectangular apertures of width a and separated by a distance d, the intensity distribution in the diffraction pattern may be represented as follows:

$$I = R_0^2 \frac{\sin^2 \beta}{\beta^2} \frac{\sin^2 N\gamma}{\sin^2 \gamma}$$

where:

$$\beta = \pi a/\lambda (\theta + i)$$

$$\gamma = \pi d/\lambda (\theta + i)$$

if we assume both the angle of diffraction, θ, and the angle of incidence, i, to be small. This expression may be further simplified by assuming a small value of a and dealing only with the central part of the diffraction pattern. In this case,

$$I = R_0^2 \frac{\sin^2 N\gamma}{\sin^2 \gamma}$$

If the angle of incidence is zero (i = 0), the intensity distribution has a principal maximum at $\theta = 0$ and other principal maxima on each side of it separated by N-1 minima and N-2 submaxima.

For example, if N = 2, the equation for the intensity distribution becomes simply:

$$I = 4 R_0^2 \cos^2 \gamma$$

and we have an intensity pattern of equally spaced maxima and minima. If N = 3, there is a single submaximum which is 11% as intense as the principal maximum. If N = 4, there are two submaxima of equal intensity, 7.4% as intense as the principal maximum. If N = 5, there are three submaxima, the center one of which is 4.0% as intense, and the outer ones 6.2% as intense, as the principal maximum.

From these examples it is observed that as N increases, the intensity of the submaxima decreases in relation to that of the principal maxima. In the case of the diffraction grating the submaxima are of essentially negligible intensity except adjacent to the principal maxima. It is important to note, however, that when N is small the submaxima are definitely visible.

These expressions and statements apply only to the patterns for a source of infinitely small dimensions, a line or point source, which assumes a single wave train being emitted from the source and diffracted. Since this is never attainable in practice, there is a problem of determining the intensity distribution in the pattern when the source has finite dimensions.

A source slit of width w is assumed, the width small in comparison to the length. This source may be divided into many line

sources of width dw. Each of these elements of source then produces its own diffraction pattern:

$$I_{dw} = R_0^2 \frac{\sin^2 N\gamma}{\sin^2 \gamma} = R_0^2 \frac{\sin^2 N\pi \frac{d}{\lambda}(\theta+i)}{\sin^2 \pi \frac{d}{\lambda}(\theta+i)}$$

and each of these will contribute to the diffraction pattern which is observed.

Let α be the angle which the source width w subtends at the diffracting apertures. It is readily seen that each element of the source has its own angle of incidence, and if the incidence angle of the center element is zero, these angles vary continuously from $-\frac{\alpha}{2}$ to $+\frac{\alpha}{2}$.

If complete incoherence is assumed for the resultant source, the intensities in the patterns produced by the source elements add.

Since the intensities are additive and the angles of incidence vary continuously from $-\frac{\alpha}{2}$ to $+\frac{\alpha}{2}$, the expression for the ensuing intensity distribution as an integral over i may be written:

$$I = R_0^2 \int_{-\alpha/2}^{\alpha/2} \frac{\sin^2 N\gamma}{\sin^2 \gamma} \, di .$$

Making use of the identity:[6]

$$\frac{\sin^2 N\gamma}{\sin^2 \gamma} = 2\left[\frac{N}{2} + (N-1)\cos 2\gamma + (N-2)\cos 4\gamma + \cdots + \cos 2(N-1)\gamma\right]$$

and the substitution: $\frac{d}{\lambda} = n$,

$$I = 2R_0^2 \int_{-\alpha/2}^{\alpha/2} \left[N/2 + (N-1)\cos 2\pi n(\theta+i) + (N-2)\cos 4\pi n(\theta+i) + \cdots + \cos 2(N-1)\pi n(\theta+i)\right] di .$$

And since cos (A+B) = cosA cosB - sinA sinB,

$$I = 2R_0^2 \int_{-\alpha/2}^{\alpha/2} \left\{ \frac{N}{2} + (N-1)(\cos 2\pi n\theta \cos 2\pi ni - \sin 2\pi n\theta \sin 2\pi ni) \right.$$

$$+ (N-2)(\cos 4\pi n\theta \cos 4\pi ni - \sin 4\pi n\theta \sin 4\pi ni) +$$

$$\ldots + \left[\cos 2(N-1)\pi n\theta \cos 2(N-1)\pi ni - \right.$$

$$\left. \left. \sin 2(N-1)\pi n\theta \sin 2(N-1)\pi ni \right] \right\} di .$$

This result when integrated term by term becomes:

$$I = 2R_0^2 \left[\frac{N\alpha}{2} + \left(\frac{N-1}{2\pi n}\right) \cos 2\pi n\theta \sin \pi n\alpha + \right.$$

$$\left(\frac{N-2}{4\pi n}\right) \cos 4\pi n\theta \sin 2\pi n\alpha + \ldots$$

$$\left. + \frac{1}{2(N-1)\pi n} \cos 2(N-1)\pi n\theta \sin (N-1)\pi n\alpha \right] .$$

This may be written as a sum:

$$I = \frac{2R_0^2}{2\pi n} \sum_{m=1}^{N-1} \left[N\pi n\alpha + \left(\frac{N-m}{m}\right) \cos 2m\pi n\theta \sin m\pi n\alpha \right] .$$

In the case of the double slit, (N = 2), this reduces to:

$$I_2 = \frac{R_0^2}{\pi n} \left[2\pi n\alpha + \cos \pi n\theta \sin \pi n\alpha \right] .$$

For complete disappearance of the fringes in this case it is necessary that $\alpha = \frac{1}{n} = \frac{\lambda}{d}$, at which value the intensity distribution is constant for all values of θ. It is also observed from

inspection of the general relation that if $\alpha = \frac{\lambda}{d}$, the intensity distribution is constant for all θ for any number of diffracting slits. This, however, gives no increase in resolving power. In order to attain such an increase it is necessary to consider the submaxima.

In general the intensity distribution is represented by a number of harmonic terms whose amplitudes depend on α. For values of α other than $\alpha = \frac{\lambda}{d}$ the intensity distribution has been obtained graphically, and a recognizable pattern has been sought to which a unique value of α could be assigned. Curves have been constructed showing the intensity distribution for various values of α for three, four, five, and six diffracting apertures.

It has been found in general that the first change in pattern takes place at $\alpha = \frac{1}{N}\frac{\lambda}{d}$. At this value of α the pattern is intermediate between the original of N-2 submaxima obtained with a line source and a pattern of N-3 submaxima. There is thus only a slight residual secondary structure.

The graphs which are shown (Figs. 1-4) are plots of intensity against the angle $\pi \frac{d}{\lambda}\theta$, the latter being taken between 0° and 180°. In all cases the lowest line is that for a line source. This is plotted to a different scale than the others, but the relative intensities remain the same. The other lines are curves of constant α, for larger values of α. For the case N = 3, Fig. 1, it is observed that all trace of the submaximum disappears at $\alpha = \frac{1}{3}\frac{\lambda}{d}$. It will be recognized that this particular value of α might be difficult to determine precisely experimentally, since beyond this the minimum merely becomes more narrow.

Fig. 1

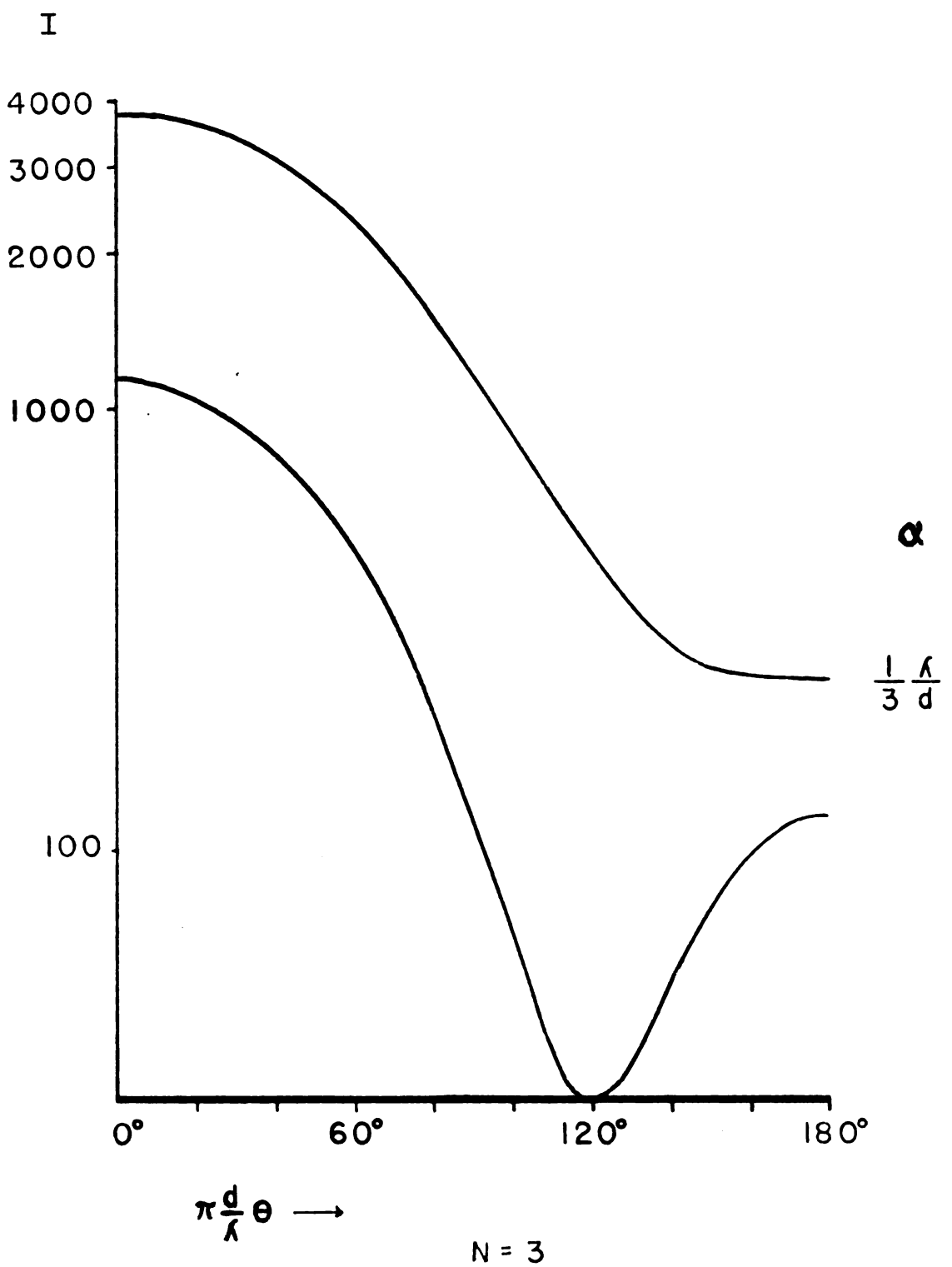

Fig. 2

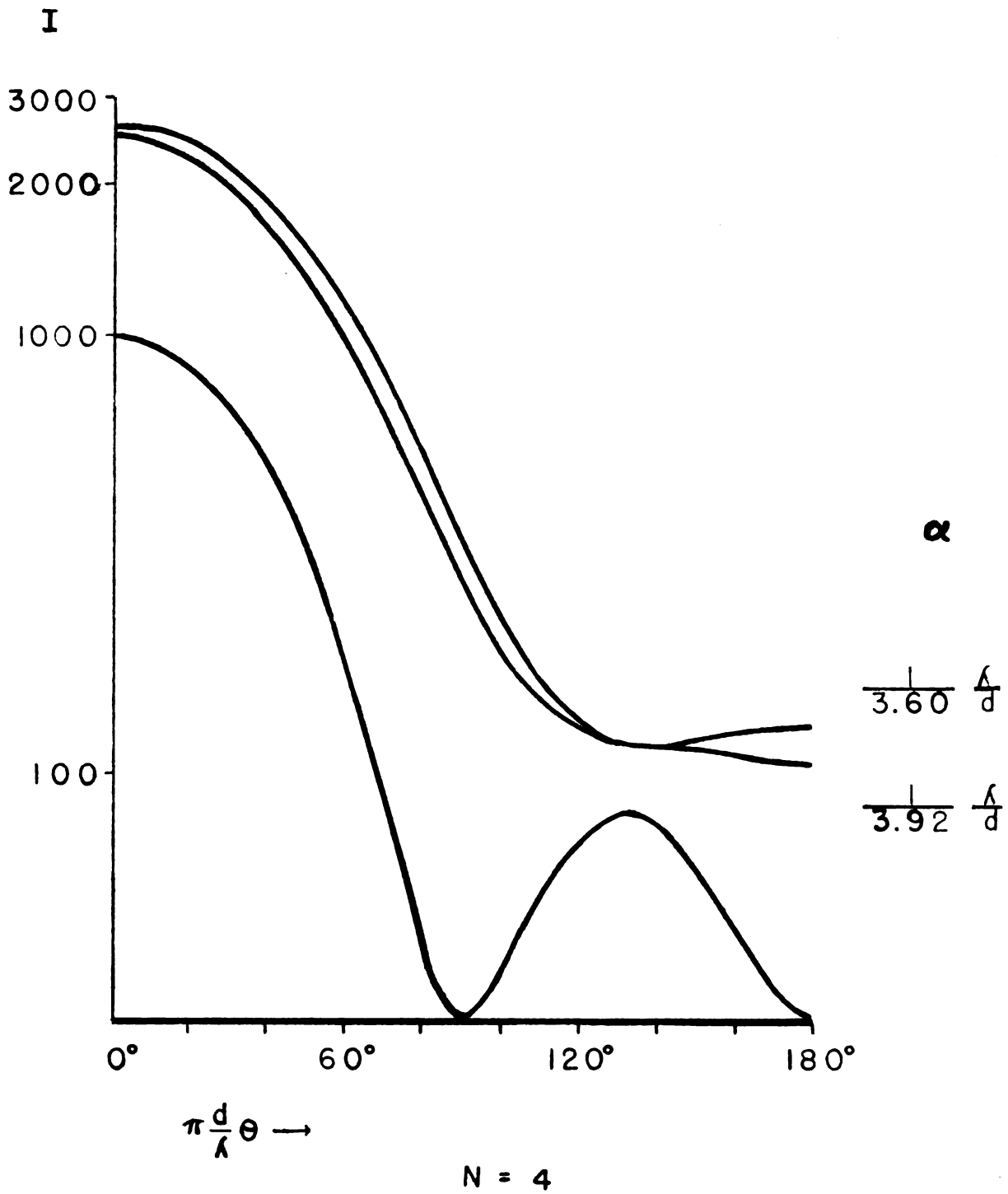
I
3000
2000
1000
100
0°
60°
120°
180°
$\pi \frac{d}{\lambda} \theta \longrightarrow$
α
$\frac{1}{3.60} \frac{\lambda}{d}$
$\frac{1}{3.92} \frac{\lambda}{d}$
N = 4

Fig. 3

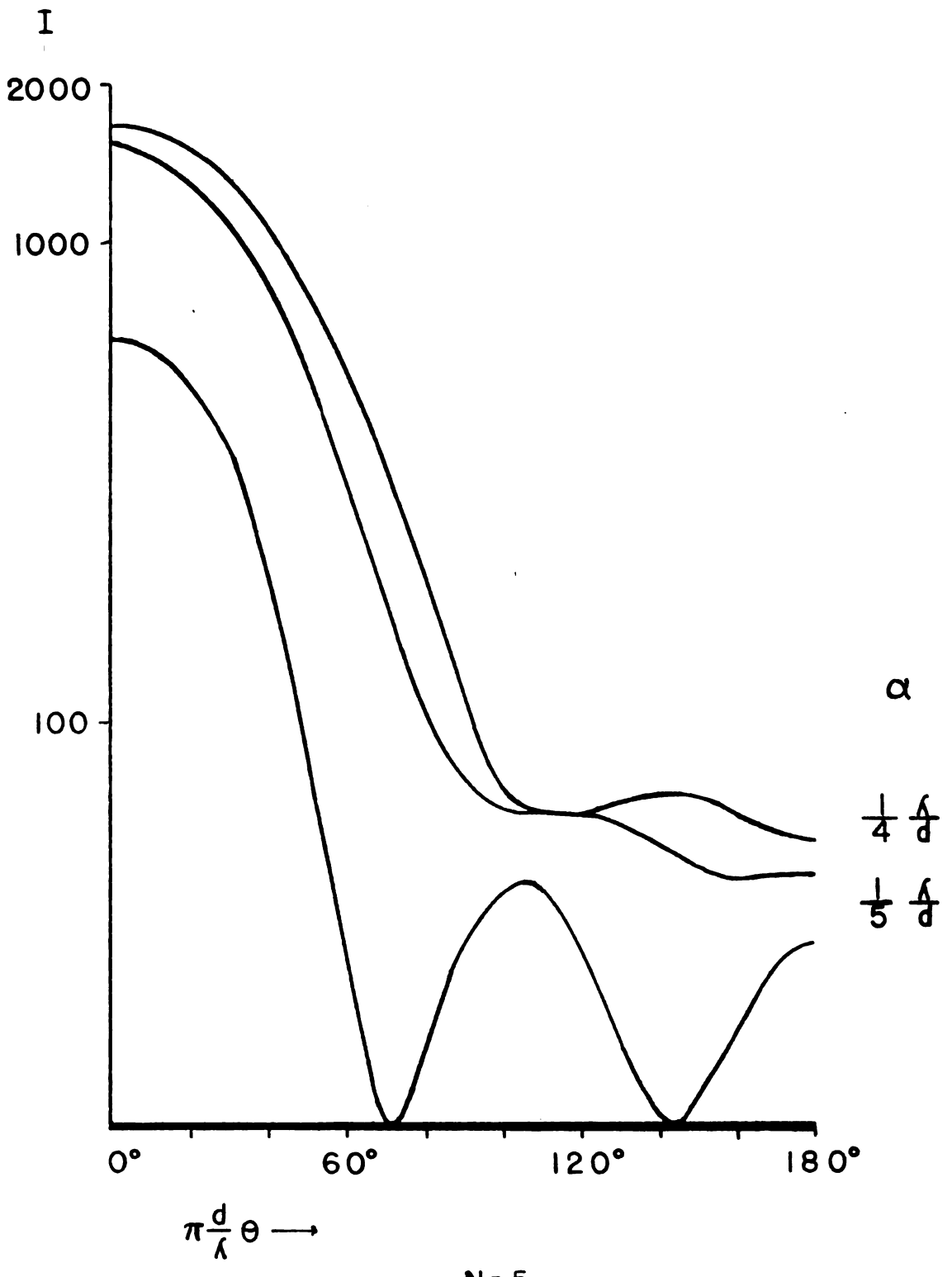

Fig. 4

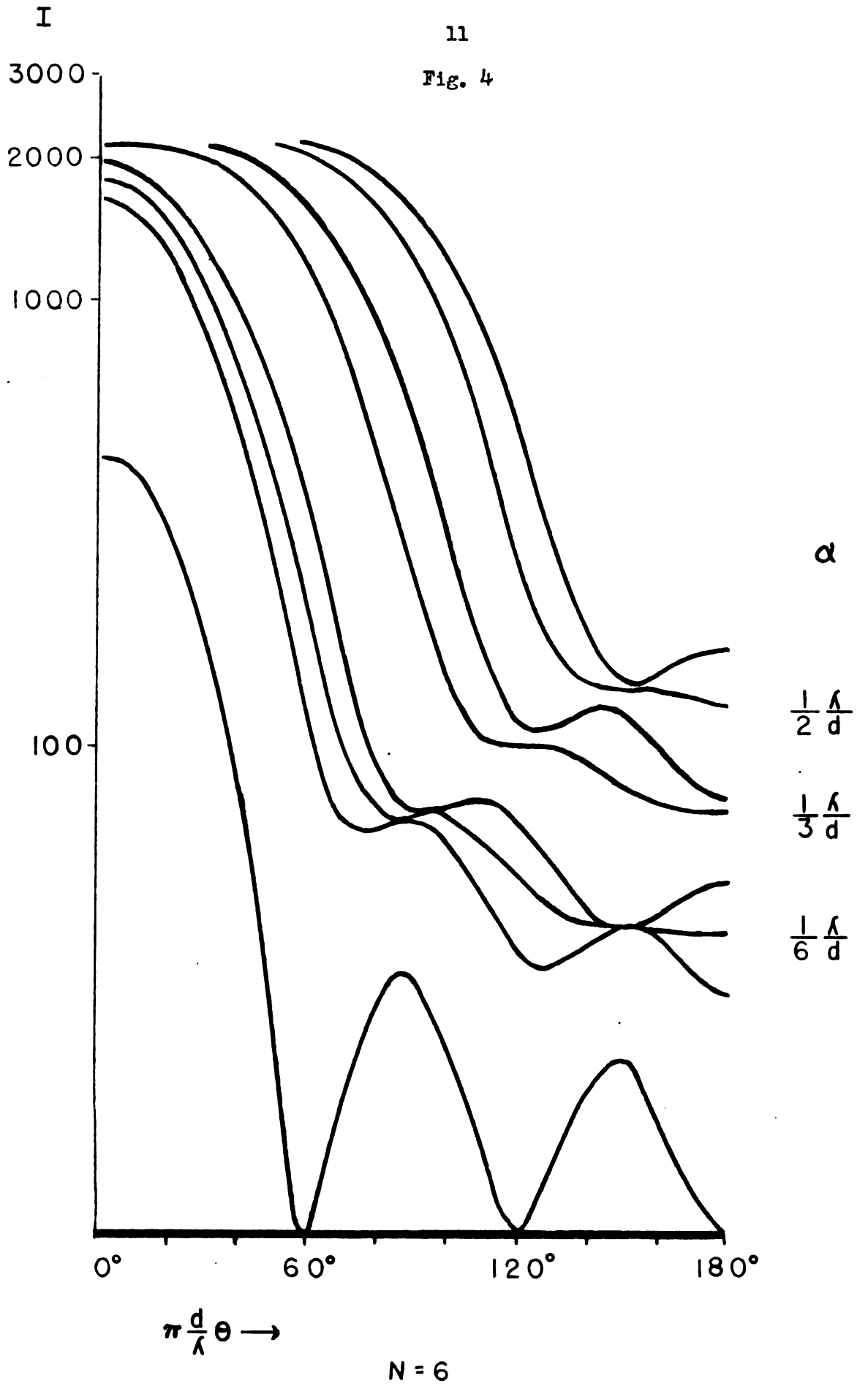

In Fig. 2, N = 4, the intensity distribution changes from one having two submaxima to a pattern having one submaximum at $\alpha = \frac{1}{3.92}\frac{\lambda}{d}$. This value is quite precise and can be successfully recognized experimentally. The deviation from the general relation $\frac{1}{N}\frac{\lambda}{d}$ is accounted for by the lack of symmetry in the intensity distribution for the small source. This lack of symmetry exists in all patterns for $N \geq 4$, but becomes negligible for higher values. Fig. 3, N = 5, follows in similar manner.

In Fig. 4, the six-slit case is carried through a greater range of α to illustrate what occurs as the source slit is widened. Changes in character of the pattern are seen to take place at $\alpha = \frac{1}{6}\frac{\lambda}{d}$, $\alpha = \frac{1}{3}\frac{\lambda}{d}$, $\alpha = \frac{1}{2}\frac{\lambda}{d}$. Not shown here is the final disappearance of all submaxima, which takes place at approximately $\alpha = \frac{1}{1.5}\frac{\lambda}{d}$. There is also a minor structure in the principal maxima which appears for $\alpha > \frac{1}{3}\frac{\lambda}{d}$.

The stated purpose here is to obtain an increase in resolving power with the overall area occupied by the diffracting slits limited to a constant value. Call this overall width s. In the two-slit case, d = s, and the disappearance of fringes takes place at $\alpha = \frac{\lambda}{s}$. When three slits are used in the same area, s = 2d and the submaximum disappears at $\alpha = \frac{2}{3}\frac{\lambda}{s}$. In general, s = (N-1)d and the change in the character of the pattern takes place when $\alpha = \frac{N-1}{N}\frac{\lambda}{s}$. This gives for N = 3 a source to which dimensions may be assigned that is two-thirds the size of source which is resolvable by the two slit, representing an increase in resolving power of 33%. In the case of N = 4, the change takes place when $\alpha = \frac{3}{3.92}\frac{\lambda}{s}$, giving an increase

in resolving power of about 23%. In general, the increase in resolving power associated with this change in pattern is $\frac{100}{N}\%$. This percentage decreases as N increases. Therefore, the greatest increase in resolving power is found when N = 3, followed by a lesser increase in N = 4, etc.

Experimentally the three slit case presents difficulty, as is expected from the graphs of intensity distribution. In the other cases the transition is limited to a very small range of values for α and may be determined quite accurately.

Experimental verification was obtained quite simply with a laboratory spectrometer. Diffracting apertures were ruled on aluminized glass plates and mounted on the spectrometer table. The bilateral slit of the collimator became the variable source slit, and the patterns were either observed visually with the telescope or photographed with an attached camera. The width of the source slit for a particular type pattern was determined by direct measurement with a microscope comparator. With apparatus available and considering the scale of the experiments, the source width could be determined with an accuracy of only 5-10% at best. In all cases, the width of source slit could be determined more precisely from the type of pattern produced than from direct measurement.

The pictures in the following pages may be compared with the preceding graphs. Figs. 5-7 are a sequence of patterns for N = 4 and may be compared with Fig. 2 for graphical description. Figs. 8-11 inclusive are the patterns for N = 6 and may be compared with the graph in Fig. 4.

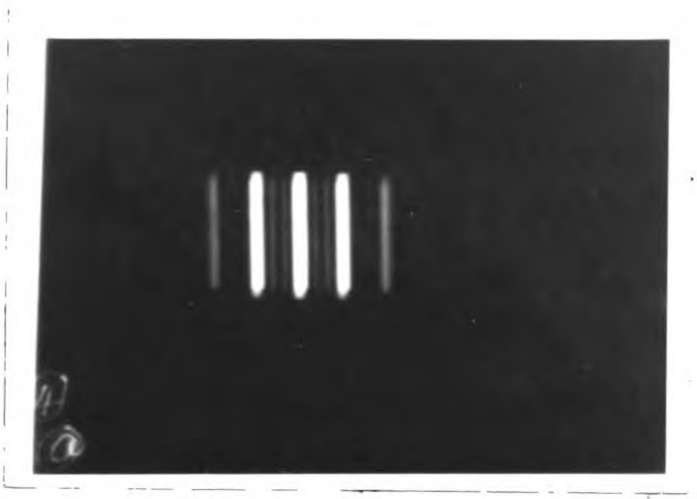

Fig. 5. N = 4. Line source.

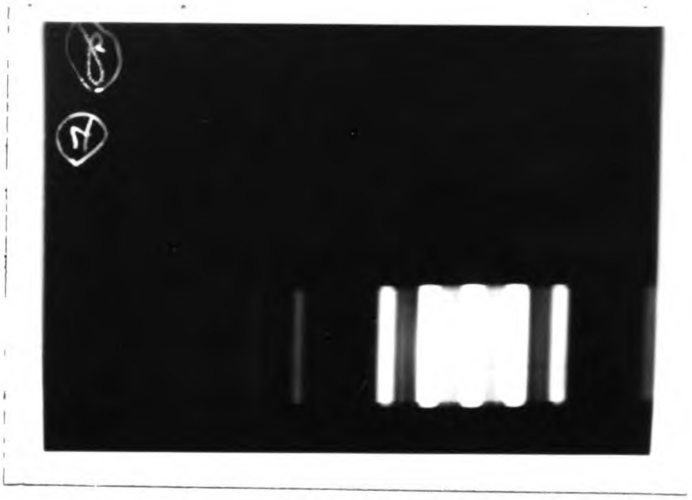

Fig. 6. N = 4.
First disappearance of submaxima:

$$\alpha = \frac{1}{3.92}\frac{\lambda}{d}.$$

By direct measurement,
w = 0.18 mm.
By calculation,
w = 0.17 mm.

Fig. 7. N = 4. Single submaximum visible.

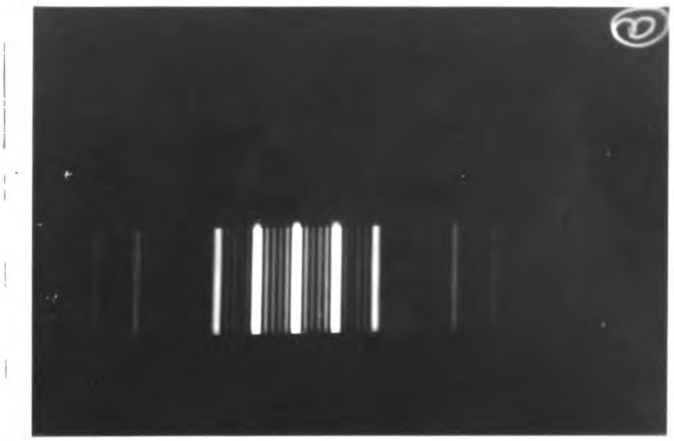

Fig. 8. N = 6. Line source.

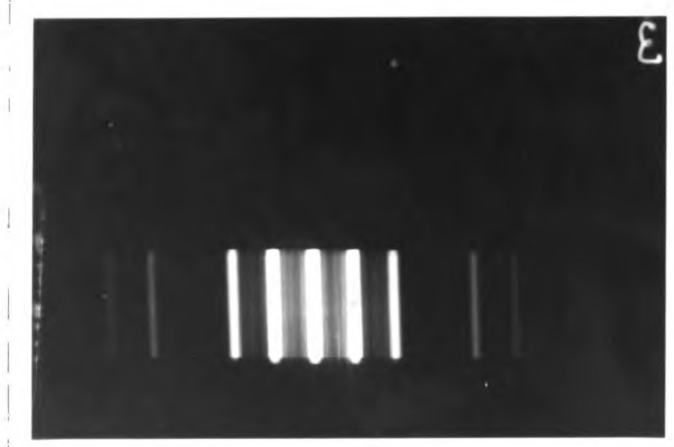

Fig. 9. N = 6.
First disappearance of submaxima:

$$\alpha = \frac{1}{6}\frac{\lambda}{d}$$

By direct measurement,
w = 0.12 mm.
By calculation,
w = 0.11 mm.

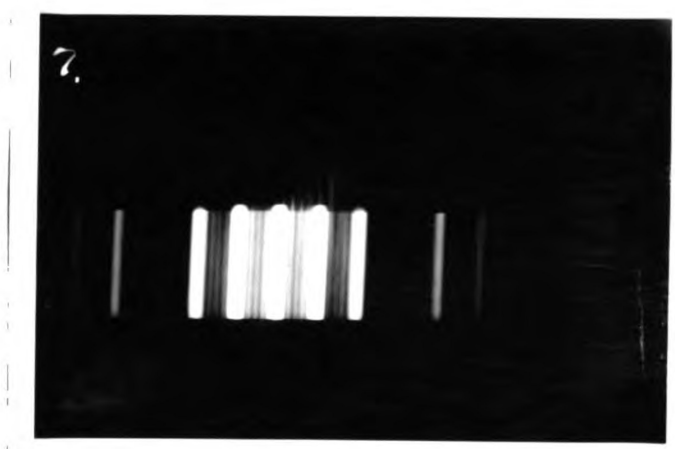

Fig. 10. N = 6.
Three submaxima visible.

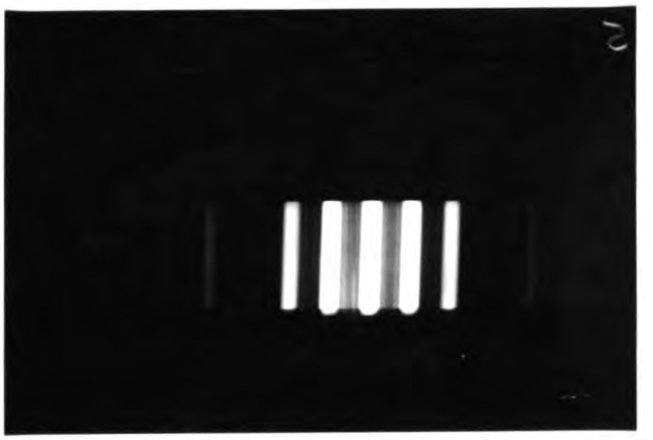

Fig. 11. N = 6.
Second disappearance of submaxima:

$$\alpha = \frac{1}{3}\frac{\lambda}{d}$$

By direct measurement,
w = 0.22 mm.
By calculation,
w = 0.22 mm.

III. DISK SOURCE

Calculations have been carried out for a circular or disk source as follows, again assuming the following expression for an infinitely small source:

$$I = R_0^2 \frac{\sin^2 N r}{\sin^2 r} .$$

In this case a disk source of finite dimensions is divided into many line sources of width dx and of length $2\sqrt{w^2-x^2}$, where w is the radius of the source and x is the distance of any element from the center.

For any element of width dx, the contribution to the diffraction pattern may be written as follows:

$$dI = f(i)\, di \frac{\sin^2 N r}{\sin^2 r} .$$

Using the same identity as for the slit source:[6]

$$dI = 2 f(i)\, di \left[\frac{N}{2} + (N-1)\cos 2\gamma + (N-2)\cos 4\gamma + \cdots + \cos 2(N-1)\gamma \right]$$

where, as before, $\gamma = \pi \frac{d}{\lambda} (\theta + i)$

and making the substitution $n = 2\pi \frac{d}{\lambda}$

$$dI = 2 f(i)\, di \left\{ \frac{N}{2} + (N-1)(\cos n\theta \cos ni - \sin n\theta \sin ni) + (N-2)(\cos 2n\theta \cos 2ni - \sin 2n\theta \sin 2ni) + \cdots + \left[\cos(N-1)n\theta \cos(N-1)ni - \sin(N-1)n\theta \sin(N-1)ni \right] \right\} di .$$

If it is assumed that the contribution of a single source element to the intensity at the center of the diffraction pattern is proportional to the area of the element, namely $2\sqrt{w^2-x^2}\, dx$, and 2α is the angle subtended by a diameter of the source at the diffracting apertures, source and diffractor being separated by a distance K,

$$w = K\alpha \quad , \quad x = Ki$$

$$f(i)\, di = 2K^2 \sqrt{\alpha^2 - i^2}\, di .$$

If these substitutions are made and the resulting expression is integrated over the entire source, the integration limits are $-\alpha$ and $+\alpha$, the resulting intensity distribution is:

$$I = 4K^2 \int_{-\alpha}^{\alpha} \left\{ \frac{N}{2} \sqrt{\alpha^2 - i^2} + (N-1)\sqrt{\alpha^2 - i^2} \left(\cos n\theta \cos ni \right. \right.$$

$$- \sin n\theta \sin ni) + (N-2)\sqrt{\alpha^2 - i^2}(\cos 2n\theta \cos 2ni$$

$$- \sin 2n\theta \sin 2ni) + \cdots + \sqrt{\alpha^2 - i^2}$$

$$\left. \left[\cos(N-1)n\theta \cos(N-1)ni - \sin(N-1)n\theta \sin(N-1)ni \right] \right\} di.$$

Since the sine terms are all odd functions they drop out of the expression and there remains

$$I = 4K^2 \int_{-\alpha}^{\alpha} \left\{ \frac{N}{2} \sqrt{\alpha^2 - i^2} + (N-1)\sqrt{\alpha^2 - i^2} \cos n\theta \cos ni \right.$$

$$+ (N-2)\sqrt{\alpha^2 - i^2} \cos 2n\theta \cos 2ni + \cdots$$

$$\left. + \sqrt{\alpha^2 - i^2} \cos(N-1)n\theta \cos(N-1)ni \right\} di$$

which is equivalent to

$$I = 8K^2 \left\{ \int_0^{\alpha} \frac{N}{2} \sqrt{\alpha^2 - i^2}\, di + (N-1)\cos n\theta \int_0^{\alpha} \cos ni \sqrt{\alpha^2 - i^2}\, di \right.$$

$$+ (N-2)\cos 2n\theta \int_0^{\alpha} \sqrt{\alpha^2 - i^2} \cos 2ni\, di + \cdots$$

$$\left. + \cos(N-1)n\theta \int_0^{\alpha} \sqrt{\alpha^2 - i^2} \cos(N-1)ni\, di \right\}$$

Further simplification is introduced by making the substitutions:

$$u = i/\alpha \quad , \quad m = n\alpha = 2\pi d/\lambda \, \alpha$$

This changes the limits since

when i = 0, u = 0
when i = d, u = 1

These substitutions give:

$$I = 8K^2\alpha^2 \left\{ \int_0^1 \frac{N}{2}\sqrt{1-u^2}\,du + (N-1)\cos n\theta \int_0^1 \sqrt{1-u^2}\cos mu\,du + (N-2)\cos 2n\theta \int_0^1 \sqrt{1-u^2}\cos 2mu\,du + \ldots + \cos(N-1)n\theta \int_0^1 \sqrt{1-u^2}\cos(N-1)mu\,du \right\}$$

Upon integration this becomes:[7]

$$I = 8K^2\alpha^2\pi/2 \left\{ \frac{N}{4} + \left(\frac{N-1}{m}\right)\cos n\theta\, J_1(m) + \left(\frac{N-2}{2m}\right)\cos 2n\theta\, J_1(2m) + \ldots + \frac{1}{(N-1)m}\cos(N-1)n\theta\, J_1[(N-1)m] \right\}$$

where $J_1(m)$ is the Bessel function of first order. This may be written:

$$I = \frac{4K^2\alpha^2\pi}{m} \sum_{l}^{N-1} \left[\frac{Nm}{4} + \left(\frac{N-l}{l}\right)\cos l n\theta\, J_1(lm) \right].$$

If this is expanded for N = 2,

$$I_2 = \frac{4K^2\alpha^2\pi}{m}\left[\frac{m}{2} + \cos n\theta\, J_1(m) \right].$$

It may be seen from this that, since $J_1(m) = 0$ when $m = 3.83$, the disappearance of fringes for the double slit takes place when $m = 3.83 = 2\,\frac{d}{\lambda}\alpha$, or $2\alpha = \frac{3.83}{\pi}\frac{\lambda}{d} = 1.22\frac{\lambda}{d}$.

Another property of the Bessel function is that the values for which it goes to zero are not simple multiples of each other. For

this reason it is seen that in the general case N 2, there is no value of α expected for which all terms beyond the constant are simultaneously zero, and therefore, there will be no value of source diameter for which the intensity is a constant for all θ .

The intensity distribution is plotted graphically for the four-slit case in the same fashion as for the slit sources. The curves showing the intensity distribution are given in Fig. 12. From these curves it is seen that the first change in character of this pattern takes place at $2\alpha = \frac{1.22}{4}\frac{\lambda}{d}$. The point of this change, however, is not as precise as for the slit source. There is a region of $\pm$ 5% surrounding this value in which there are no graphically visible submaxima.

Photographs of these patterns have been made and are shown in Figs. 13-18. There are two series, the first consisting of a source of constant diameter with the separation of the diffracting apertures varied, the second, a constant aperture separation with the source diameter varied.

Fig.12

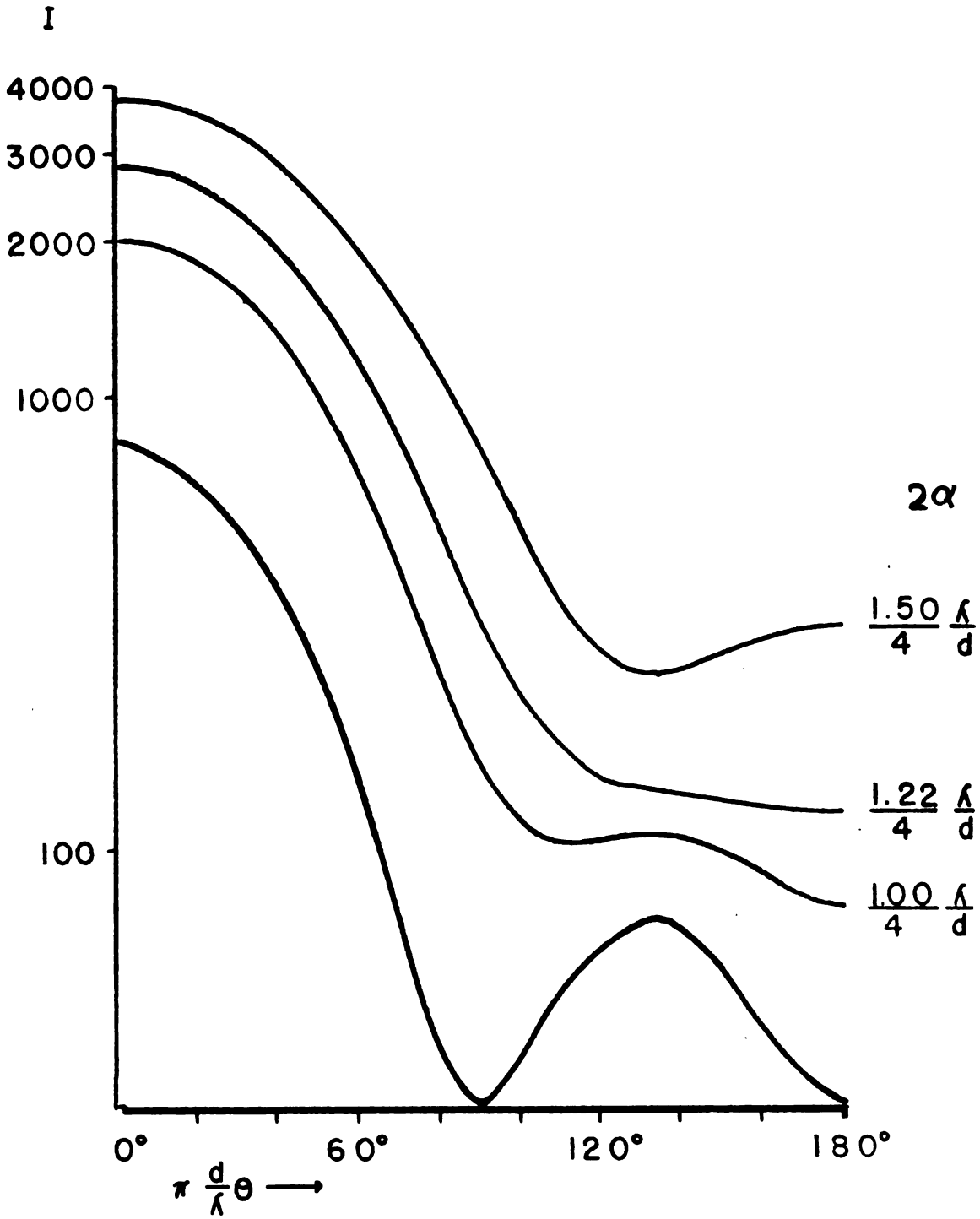

CIRCULAR SOURCE

N = 4

Constant Source Diameter

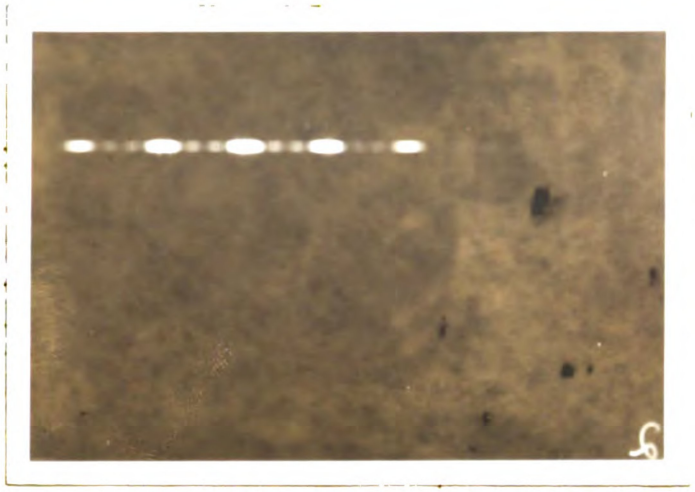

Fig. 13. Disk Source.
N = 4.
Source diameter = 0.23 mm.
Separation of apertures
= 0.16 mm.

$$2\alpha < \frac{1.22}{4}\frac{\lambda}{d}$$

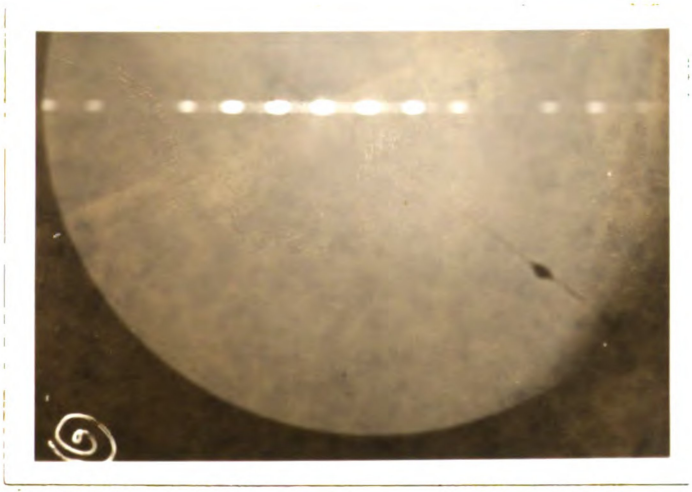

Fig. 14. Disk Source.
Source diameter = 0.23 mm.
Separation of apertures
= 0.18 mm.

$$2\alpha = \frac{1.22}{4}\frac{\lambda}{d}$$

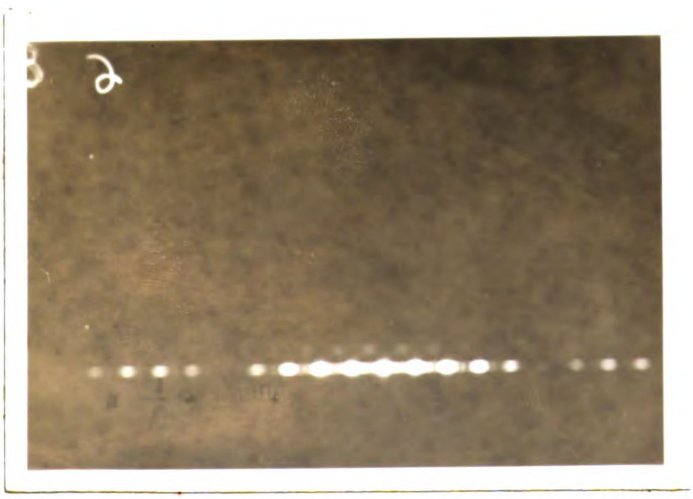

Fig. 15. Disk Source.
Source diameter = 0.23 mm.
Separation of apertures
= 0.25 mm.

$$2\alpha > \frac{1.22}{4}\frac{\lambda}{d}$$

Constant Separation of Diffracting Slits

Fig. 16. Disk Source.
N = 4
Source diameter = 0.23 mm.
Separation of apertures
= 0.10 mm.

$$2\alpha < \frac{1.22}{4}\frac{\lambda}{d}$$

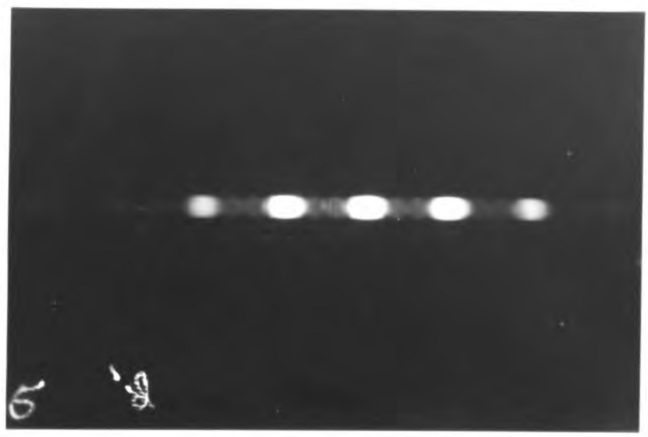

Fig. 17. Disk Source.
Source diameter = 0.42 mm.
Separation of apertures
= 0.10 mm.

$$2\alpha = \frac{1.22}{4}\frac{\lambda}{d}$$

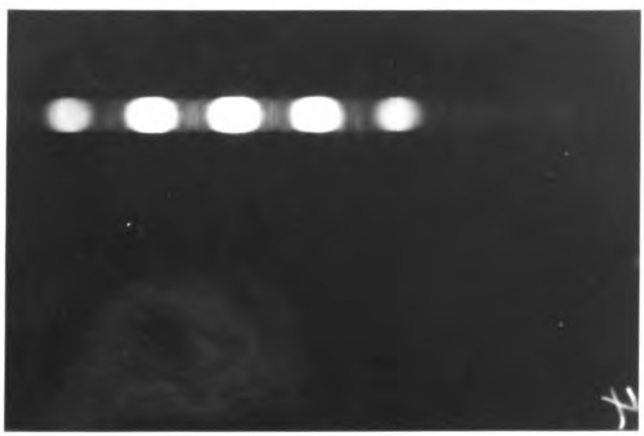

Fig. 18. Disk Source.
Source diameter = 0.66 mm.
Separation of apertures
= 0.10 mm.

$$2\alpha > \frac{1.22}{4}\frac{\lambda}{d}$$

REFERENCES

[1]Michelson, A. A., "On the Application of Interference Methods to Astronomical Methods," Phil. Mag., 30 (1890), p. 1

[2]Anderson, J. A., "Application of Michelson's Interferometer Method to the Measurement of Close Double Stars," Astrophys. Jour., 51 (1920), p. 263

[3]Michelson, A. A., "On the Application of Interferometer Methods to Astronomical Measurement," Astrophys. Jour., 51 (1920), p. 257

Michelson, A. A., and Pease, F. G., "Measurement of the Diameter of α Orionis with the Interferometer," Astrophys. Jour., 53 (1921), p. 249

[4]Gerhardt, U., "Application of the Michelson Stellar Interferometer to the Measurement of Small Particles," Zeits. f. Physik, 35 (1926), p. 697.

Gerhardt, U., and Baeyer, O. v. "Lower Limit of the Michelson Stellar Interferometer Method of Measurement," Zeits. f. Physik, 35 (1926), p. 718.

[5]Jenkins, F. A., and White, H. E., Fundamentals of Physical Optics, New York, McGraw Hill Co. Inc., 1937

[6]Jackson, D., Fourier Series and Orthogonal Polynomials, The Mathematical Association of America, 1941, p. 33, 34.

[7]Gray, A., Mathews, G. B., and MacRoberts, T. M., A Treatise on Bessel Functions, London, Macmillan and Co. Ltd., 1931, p. 46.